Journal of Medicinal Chemistry

Article

pubs.acs.org/jmc

DUPA Conjugation of a Cytotoxic Indenoisoquinoline Topoisomerase I Inhibitor for Selective Prostate Cancer Cell Targeting

Jyoti Roy,[‡,§] Trung Xuan Nguyen,[†,§] Ananda Kumar Kanduluru,[‡] Chelvam Venkatesh,[‡] Wei Lv,[†] P. V. Narasimha Reddy,[†] Philip S. Low,[‡] and Mark Cushman*[,†]

[†]Department of Medicinal Chemistry and Molecular Pharmacology, College of Pharmacy, and the Purdue Center for Cancer Research, Purdue University, West Lafayette, Indiana 47907, United States

[‡]Department of Chemistry, College of Science, Purdue University, West Lafayette, Indiana 47907, United States

Supporting Information

ABSTRACT: Prostate-specific membrane antigen (PSMA) is overexpressed in most prostate cancer cells while being present at low or undetectable levels in normal cells. This difference provides an opportunity to selectively deliver cytotoxic drugs to prostate cancer cells while sparing normal cells that lack PSMA, thus improving potencies and reducing toxicities. PSMA has high affinity for 2-[3-(1,3-dicarboxypropyl)ureido]pentanedioic acid (DUPA) (K_i = 8 nM). After binding to a DUPA–drug conjugate, PSMA internalizes, unloads the conjugate, and returns to the surface. In the present studies, an indenoisoquinoline topoisomerase I inhibitor was conjugated to DUPA via a peptide linker and a drug-release segment that facilitates intracellular cleavage to liberate the drug cargo. The DUPA–indenoisoquinoline conjugate exhibited an IC_{50} in the low nanomolar range in 22RV1 cell cultures and induced a complete cessation of tumor growth with no toxicity, as determined by loss of body weight and death of treated mice.

INTRODUCTION

Prostate cancer (PCa) is the second most frequent cause of cancer mortality in men in the United States (following lung cancer as number one) with an estimated 233 000 new cases and 29 480 deaths in 2014.[1] Commonly elected strategies to effectively treat PCa involve surgery, radiation, hormonal therapy, and chemotherapy. Unfortunately, the use of anticancer drugs is associated with the development of tumor resistance and adverse effects that compromise their usefulness.[2,3] Therefore, there is a critical need for safer and more effective methods for treatment of PCa.

Most PCa cells overexpress prostate-specific membrane antigen (PSMA) compared to the restricted expression pattern observed in normal prostate cells.[4] Low PSMA expression is also found in other normal tissue types including kidney, the intestinal brush border membrane, and brain.[4−6] Gene array analysis and immunohistochemistry studies have revealed that PSMA is the second most up-regulated protein in PCa, and the expression level rises with the aggressiveness of the cancer.[7] PSMA is also highly overexpressed in the neovasculature of solid tumors,[8,9] especially as the tumor progresses or metastasizes.[8] The difference in PSMA expression between prostate cancer cells and normal cells offers an opportunity to selectively deliver nonspecific cytotoxic drugs to PCa cells while sparing healthy cells.

PSMA (also called folate hydrolase I or glutamate carboxypeptidase II) has high affinity for 2-[3-(1,3-dicarboxypropyl)ureido]pentanedioic acid (DUPA, **1**) (K_i = 8 nM, IC_{50} = 47 nM).[10,11] Upon binding to a ligand (e.g., DUPA), PSMA undergoes endocytosis through clathrin-coated pits, unloads the ligand, and then recycles rapidly to the cell surface.[12] These properties make PSMA an excellent candidate for tumor-targeted drug delivery of anticancer agents.[13−15]

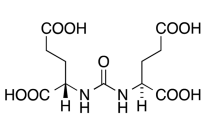

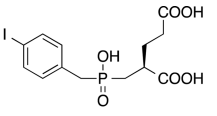

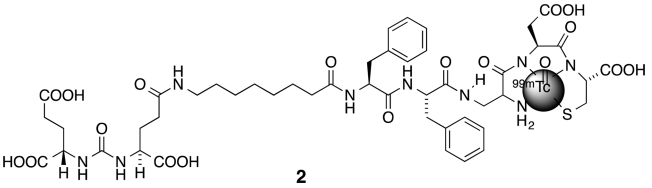

In 2009, the Post and Low groups at Purdue University reported the design of a ^{99m}Tc-radioimaging derivative **2** of DUPA starting from the crystal structure of a PSMA–inhibitor **3** complex (PDB code 2C6C).[16] The radioimaging agent has potential applications in detecting prostate cancer recurrence, monitoring response to therapy, and selecting patients for PSMA-targeted therapy.[15] Subsequent studies demonstrated that DUPA-linked cytotoxic drugs such as tubulysin B hydrazide and desacetyl vinblastine hydrazide are able to eradicate tumor in vivo and eliminate nonspecific toxicity associated with the unconjugated drugs.[14]

Received: November 27, 2014

DOI: 10.1021/jm5018384
J. Med. Chem. XXXX, XXX, XXX−XXX

DRUG DESIGN

Since PSMA is only expressed at the level of about one million copies per prostate cancer cell,[13] one must consider only very potent and highly cytotoxic anticancer drugs for DUPA conjugation so that the low concentrations that get delivered inside prostate cancer cells using PSMA as a shuttle can still be effective. The indenoisoquinoline **4** was obtained as part of a program to synthesize potential metabolites of indotecan (**5**, aka LMP400) (Figure 1) and the related anticancer drug

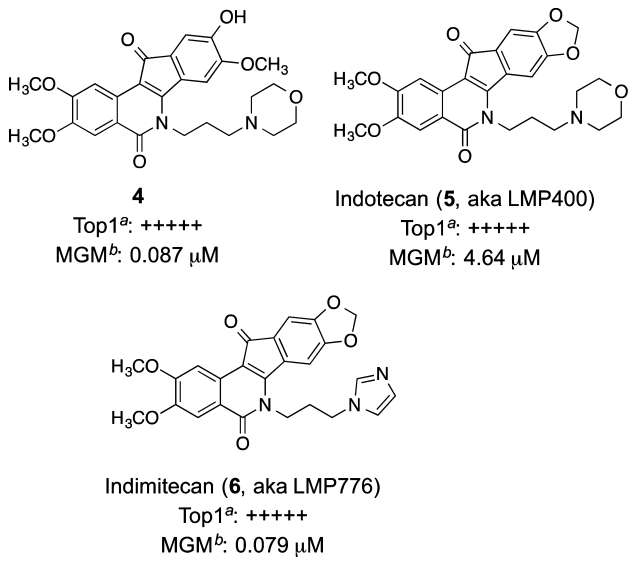

Figure 1. Candidate Top1 inhibitor **4** for DUPA conjugation. [a]Top1 inhibitory activity in the Top1-mediated DNA cleavage assay is graded on the following rubric relative to 1 μM camptothecin: 0, no inhibitory activity; +, between 20% and 50% activity; ++, between 50% and 75% activity; +++, between 75% and 95% activity; ++++, equipotent; ++++ +, more potent. The activity is a semiquantitative estimate of the sum of the intensities of the DNA cleavage bands observed in the polyacrylamide electrophoresis gel.[17] [b]The mean-graph midpoint (MGM) is an approximate average of the GI_{50} values obtained across the entire NCI panel of 60 human cancer cell lines successfully tested, where during the MGM calculation, compounds with GI_{50} values that fall outside the testing range of 0.01−100 μM are assigned values of 0.01 and 100 μM.[17]

indimitecan (**6**, aka LMP776) in order to obtain structurally defined synthetic standards that could be used to elucidate the structures of the actual metabolites.[17] Although it was not one of the metabolites, the indenoisoquinoline **4** was found to possess very potent topoisomerase I inhibitory activity (+++++; see Figure 1 legend) and cytotoxicity [mean-graph midpoint (MGM) GI_{50} = 87 nM in the NCI's panel of 60 human cancer cell cultures].

The unexpectedly high activity of **4** led to the realization that the phenol functionality provided an unanticipated opportunity to target a very potent indenoisoquinoline to prostate cancer cells by removing the technetium from the imaging agent **2** and installing the indenoisoquinoline in its place as shown in Scheme 1, a strategy that has proven to be successful with other anticancer drugs.[13] The indenoisoquinoline **4** was therefore selected for use in the present studies as the candidate to test our targeting hypothesis and provide preliminary data for future drug development.

The release mechanism is proposed to involve disulfide reduction by glutathione within the reducing environment of the endosomes to yield intermediate **8** (Scheme 1).[18] The sulfhydryl group in the intermediate **8** is positioned to carry out an intramolecular nucleophilic attack to liberate **4** and form ethylene sulfide **9** and carbon dioxide (major route) or 1,3-oxathiolan-2-one (**10**, minor route).[13] Previous studies of the efficiency of the disulfide reduction in DUPA conjugates by HPLC and LC/MS revealed over 98% reduction in 2−4 h upon addition of a 10-fold excess of glutathione.[13]

The design of the conjugate **7** was facilitated by molecular modeling of its complex with PSMA (Figure 2). The docking and energy minimization procedure used to construct this model can be summarized in the following steps: (1) the conformation of DUPA was energy minimized by Sybyl and then docked into the ligand binding site of PSMA (PDB code 2C6C), with the original ligand GPI-18431 removed using GOLD 3.0; (2) the conformation of the linker peptide was energy minimized by Sybyl and then linked to DUPA through a covalent bond and docked into the PSMA binding site using GOLD 3.0; (3) the conformation of the indenoisoquinoline was energy minimized by Sybyl and then linked to the peptide through a covalent bond and docked to the PSMA binding site using GOLD 3.0; (4) further energy minimization of the resulting conjugate **7**−PSMA complex was performed with Sybyl. For the protein, AMBER charges were used. For the ligand, Gasteiger charges were used, and the minimization of the conjugate−PSMA complex was performed with the AMBER7FF99 force field.

According to the molecular model of **7** bound to PSMA displayed in Figure 2, the DUPA fragment on the right side of the conjugate and the connected polymethylene linker occupy a tunnel shown here in the center of the protein. The conjugate structure emerges from the tunnel at the level of the two phenylalanines, and the remaining structure pointing to the left has protein on one side but is essentially open to the bulk solvent on the other side (which faces the viewer). Overall, the model indicates that the prodrug **7** fits PMSA nicely, with no obvious unfavorable interactions.

SYNTHESIS

As depicted in Scheme 2, Fmoc solid-phase peptide synthesis was used to prepare the DUPA−peptide reagent **12**. The reported procedure[15] was modified to optimize the reaction yield and time efficiency. The reported procedure[15] used Fmoc-Cys(Trt)-(4-MeOTrt) resin, which has been found in some cases to cause racemization of L-Cys to D-Cys. Therefore, the current methodology employed the Fmoc-free H-Cys(Trt)-(2-ClTrt) resin (**11**) instead, which saves time that the first Fmoc-cleavage would have taken if the Fmoc-Cys(Trt)-(4-MeOTrt) resin had been used and might also be expected to suppress racemization.[19] The procedure for the final cleavage of the DUPA−peptide from the resin was modified slightly to maximize the yield.

Scheme 3 shows the synthesis of the protected DUPA reagent **17**.[11,15] α,γ-Di-*tert*-butyl glutamate **13** was treated with triphosgene in the presence of Et_3N at 0 °C for 2 h to provide the isocyanate **14**. Addition of glutamate **15**, bearing benzyl protection on the γ-carboxylate and a *tert*-butyl protecting group on the α-carboxylate, with overnight stirring, yielded the protected urea **16** after workup and chromatographic purification. Atmospheric hydrogenation of **16** in EtOAc for 2 days in the presence of Pd−C afforded the pure DUPA precursor **17** in 100% yield.

DOI: 10.1021/jm5018384
J. Med. Chem. XXXX, XXX, XXX−XXX

Scheme 1

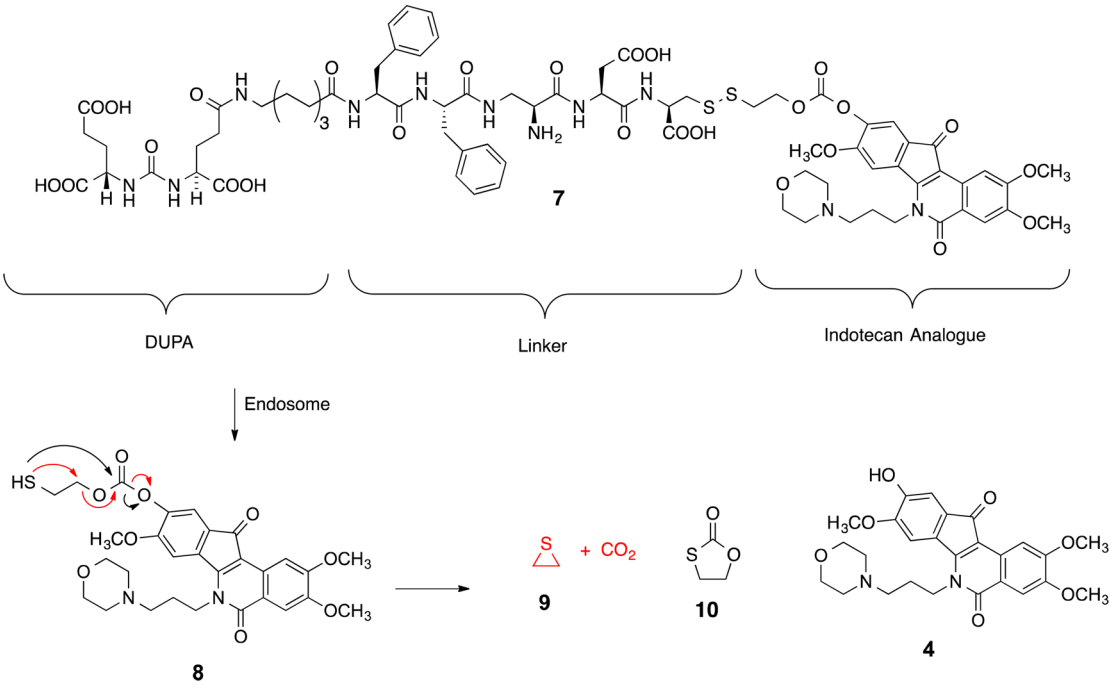

The synthesis of the desired DUPA–indenoisoquinoline carbonate conjugate **7** is shown in Scheme 4. Reaction of the phenol **4**[17] with carbonate reagent **18** yielded the carbonate **19**. Treatment of **19** with the DUPA–peptide reagent **12** in DMSO and DIPEA at room temperature overnight afforded the DUPA–indenoisoquinoline carbonate conjugate **7**.

The synthesis of the carbonate reagent **18** is outlined in Scheme 5.[13] Treatment of 2-mercaptoethanol (**20**) with sulfenyl chloride **21**, followed by a disulfide exchange with pyridine **22** in CH_3CN at reflux, provided alcohol **23** as a hydrochloride salt. Reaction of **23** with triphosgene (**24**) afforded an intermediate that upon ester exchange with the hydroxybenzotriazole **25** yielded the desired carbonate reagent **18**. The syntheses reported in Schemes 2, 3, and 5 were modified slightly from the reported procedures[11,13,15] in order to improve purity, yield, ease of workup, and time efficiency.

BIOLOGICAL EVALUATION

The cytotoxicities of the free drug **4** and its DUPA conjugate **7** were evaluated in 22RV1 cell culture, and the IC_{50} values were quantified in dose-dependent ^{3}H-thymidine incorporation assays to be in the low nanomolar range (representative graphs are depicted in Figure 3). The IC_{50} value of the indenoisoquinoline **4** itself was 2.0 nM when determined after a 2 h incubation. The conjugate **7** showed no activity after a 2 h incubation, but it produced an IC_{50} value of 11.4 nM after a 24 h incubation. The conjugate **7** was slightly less potent than the drug **4** itself. However, the potential value of cancer cell targeting by the conjugate **7** would be derived from its lack of cytotoxicity in "normal" cells, which might result in **7** being a less toxic anticancer drug than **4**.

In order to demonstrate efficacy and investigate toxicity in an animal model, 22RV1 xenograft-bearing mice were treated with the indenoisoquinoline **4** or its DUPA conjugate **7** at a dose of 40 nmol/mouse (2.0 μmol/kg) by ip injection with a single dose on alternate days, 3 days/week for 3 weeks (9 doses in total) (Figure 4). Four groups of mice were utilized in the experiment: (1) the untreated group (blue) received saline and served as the control; (2) the free-drug group (green) was treated with the free drug **4**; (3) the treated group (purple) was given the DUPA conjugate **7**; (4) the competitor group (red) received both the DUPA conjugate **7** and the DUPA–peptide reagent **12**, whose concentration was in 100-fold excess of **7**. The reagent **12** served as a PSMA competitor and was used in a much higher concentration in order to completely saturate all PSMA available for DUPA-binding, thus preventing the PSMA-mediated uptake of the DUPA conjugate **7** if the uptake of **7** is in fact PSMA-mediated.

Figure 4A shows complete cessation and regression of tumor growth during the treatment period for the DUPA conjugate-treated (purple line) and free drug-treated (green line) groups, respectively, as compared to the untreated group (blue line) or the group treated with the DUPA conjugate **7** and the PSMA competitor **12** (red line). When tested at the same dose of 2.0 μmol/kg, the lesser antitumor efficacy of conjugate **7** (cessation of tumor growth) as compared to the free drug **4** (regression of tumor growth) was compensated for by the lower toxicity of the conjugate **7** (Figure 4C). Evidently, the conjugate **7** is selectively cytotoxic to prostate cancer cells vs the other cells in the body, resulting in no deaths, whereas free drug **4** resulted in the deaths of four out of the five animals during the treatment period (Figure 4C) at the relatively high dose tested. The complete loss of activity in the competition group when the PSMA competitor **12** was used in 100-fold excess of the conjugate **7**, as compared to the treated group, suggested that **12** competed with and effectively prevented **7** from binding to PSMA, thereby blocking cellular uptake of **7**. This observation indicates (1) sufficient stability of conjugate **7** in solution before cellular uptake, (2) the PSMA-mediated uptake of **7** to tumor cells, and (3) sufficient lability of **7** to enable rapid liberation of free drug **4** following internalization into the malignant cells. In another words, the data implied that the prostate cancer cell-killing effect of conjugate **7** required the presence of an empty PSMA receptor and did not occur by

DOI: 10.1021/jm5018384
J. Med. Chem. XXXX, XXX, XXX–XXX

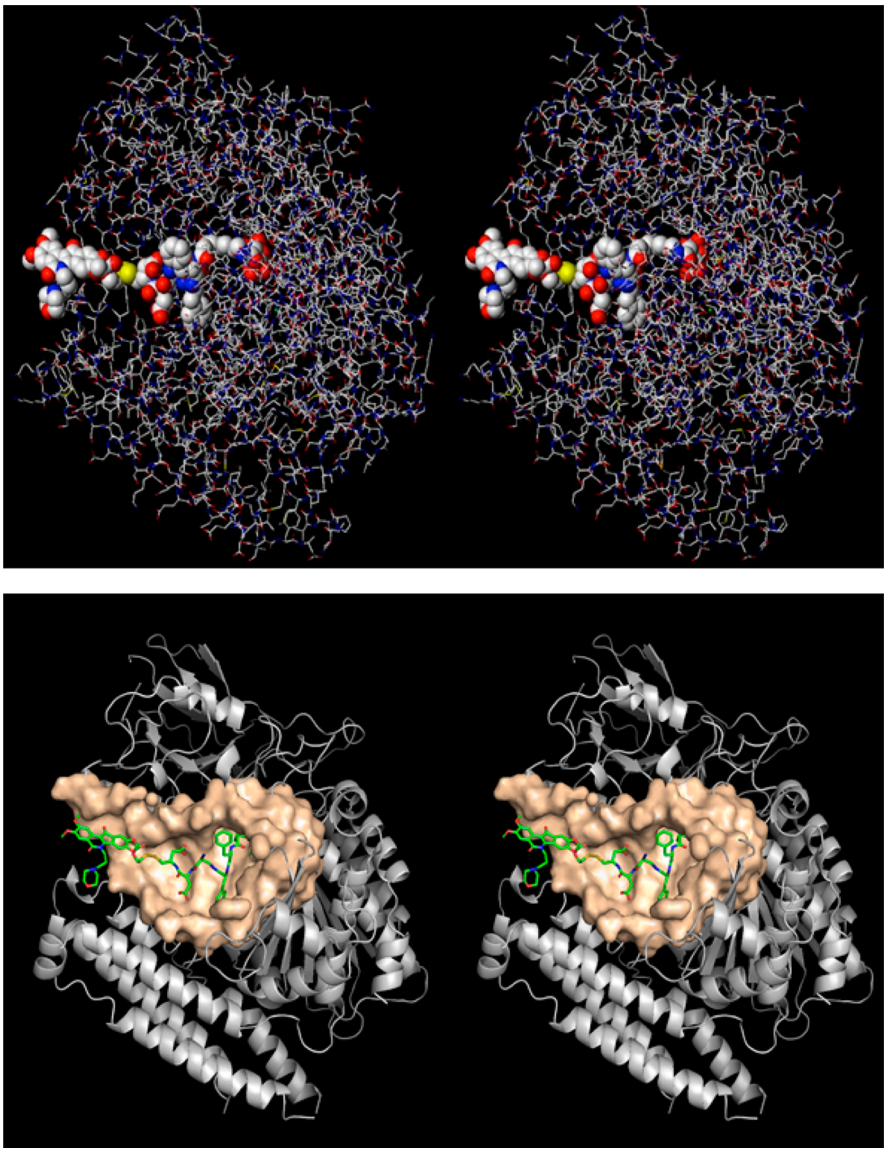

Figure 2. Molecular model of the DUPA−indenoisoquinoline conjugate **7** bound to PSMA. The stereoview is programmed for wall-eyed (relaxed) viewing. Top: ligand, space-filling model; protein, stick model. Bottom: ligand, stick model; protein, ribbon and space-filling model.

premature extracellular release of the free drug followed by passive diffusion into the diseased cells. Finally, the data in Figure 4A also document tumor regression at a high dose of the free drug **4**. Figure 4B shows that all live mice in the four groups retained their normal body weights during the treatment period and indicates that the DUPA conjugate therapy was well tolerated. The greatly reduced toxicity of **7** vs **4** (Figure 4C) supports the hypothesis that the conjugate would have greater safety and selectivity than the unconjugated drug itself. H&E staining was performed on excised tumors (Figure 5) to determine whether the residual mass left in mice after treatment comprised predominately cancer or stromal cells instead of leftover Matrigel. This confirmed that the residual lesion was comprised mostly of cancer cells.

CONCLUSION

Clinical applications of many of the available cytotoxic anticancer drugs are currently limited by two factors: (1) unacceptable toxicities and (2) the emergence of tumor resistance. Ligand-targeted therapeutics take advantage of the overexpression of a membrane receptor in rapidly proliferating cancer cells, a phenomenon that is generally more common than the expression of an up-regulated enzyme or pathway in a pathological cell. In this approach, the conversion of a cytotoxic drug to a prodrug that is specifically targeted to tumor cells by attachment of a homing ligand offers an innovative way to create anticancer agents with maximized antitumor efficacies and minimized undesirable side effects.

The current report presents DUPA conjugation of an indenoisoquinoline Top1 inhibitor as an effective general method to safely and selectively deliver indenoisoquinolines to prostate cancer cells. The prostate-targeting ligand DUPA was linked to the potent, cytotoxic Top1 inhibitor **4** (IC_{50} of 2.0 nM against 22RV1 cells) via a disulfide linker for drug release and a peptide linker that ensures the binding of DUPA to its receptor (PSMA) and improves the overall water solubility of the conjugate. In contrast to the free drug **4**, the conjugate **7** was not lethal at the effective dose tested (2 μmol/kg). In addition, experimental results indicated that the uptake of the DUPA conjugate **7** was mediated by PSMA and that **7**

DOI: 10.1021/jm5018384
J. Med. Chem. XXXX, XXX, XXX−XXX

Scheme 2[a]

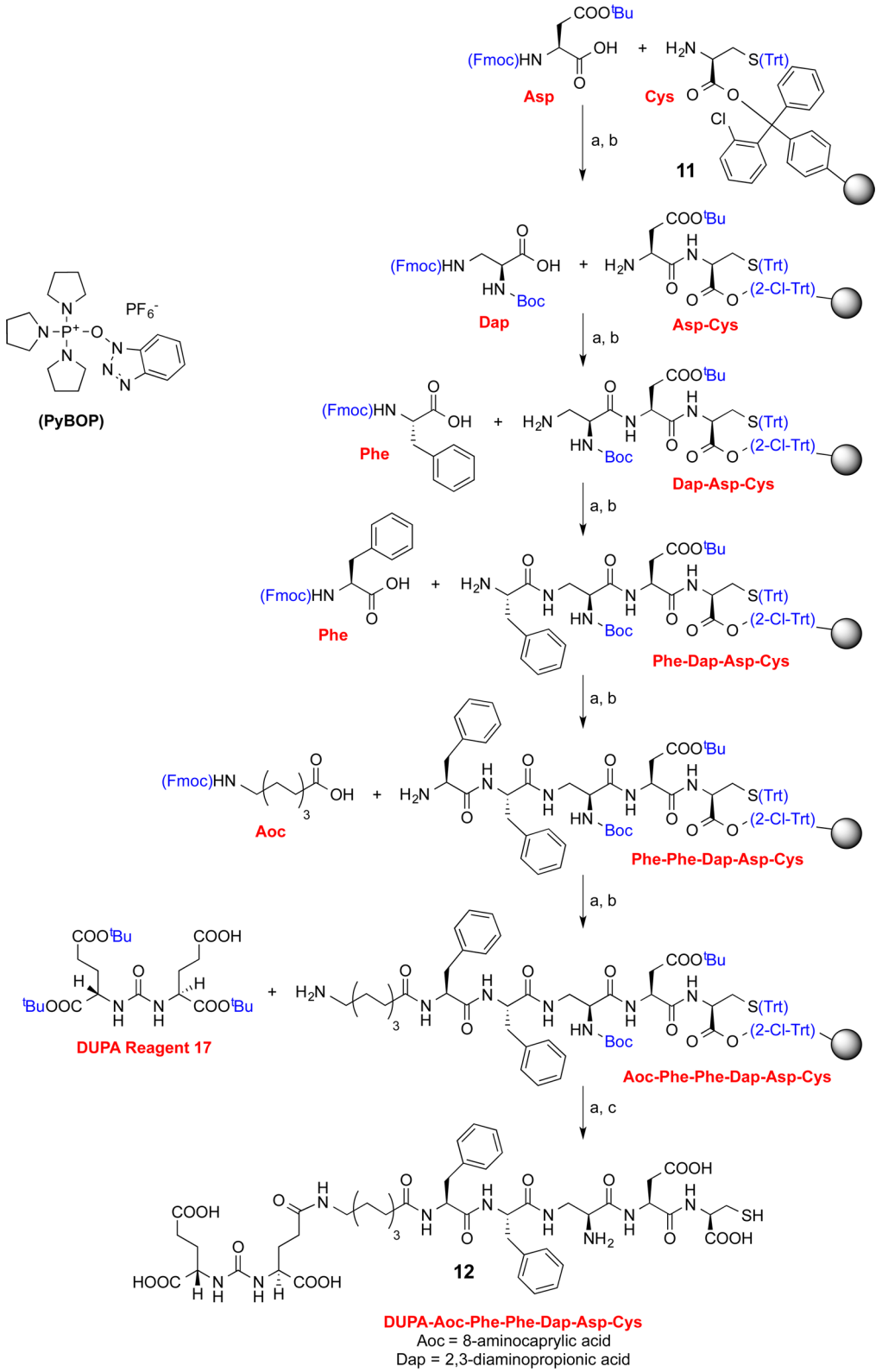

[a]Reagents and conditions: (a) PyBOP, DIPEA, DMF, 23 °C, 3 h; (b) 20% piperidine/DMF, 23 °C, 30 min; (c) TFA/H_2O/TIPS/EDT (92.5:2.5:2.5:2.5), 23 °C, 30 min.

dissolved easily in water at room temperature while free drug **4** exhibited poor aqueous solubility. Furthermore, the DUPA-targeting mechanism has also been incorporated in a ^{99m}Tc radioimaging agent **2** that can be used in conjunction with the DUPA conjugate **7** to locate and monitor response to therapy and identify patients who are suitable for the DUPA–indenoisoquinoline Top1 inhibitor treatment.[14,15] Lastly, the unique characteristics of PSMA (expression level rises with

DOI: 10.1021/jm5018384
J. Med. Chem. XXXX, XXX, XXX−XXX

Scheme 3

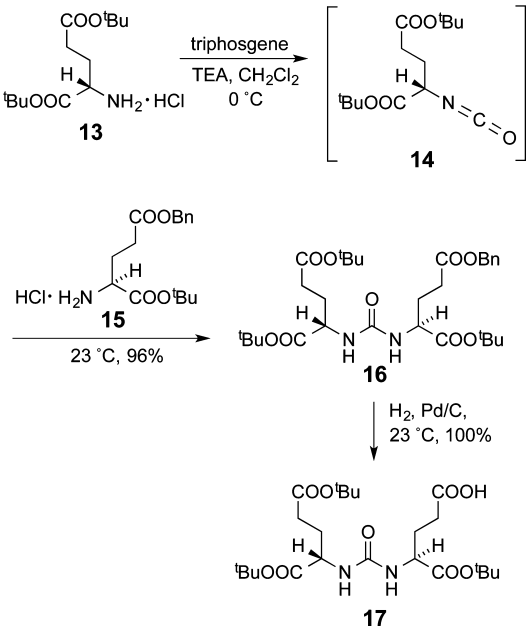

Scheme 4

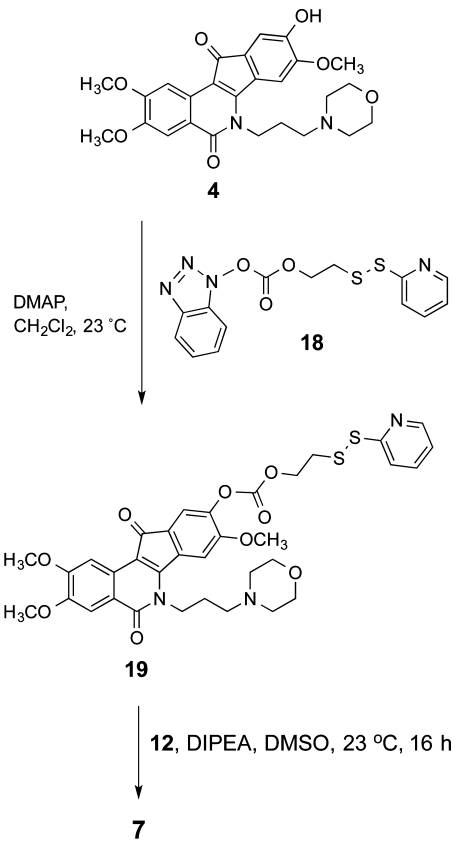

tumor aggressiveness, and it is present at all tumor stages and is up-regulated following androgen withdrawal) render it a useful therapeutic target for chemotherapy, which, along with the current conjugation approach, may provide new and effective drugs for the treatment and cure of metastatic prostate cancer without causing unacceptable, dose-limiting toxic effects.

It is likely that the most challenging problems that will be encountered in future drug design of indenoisoquinoline–

Scheme 5

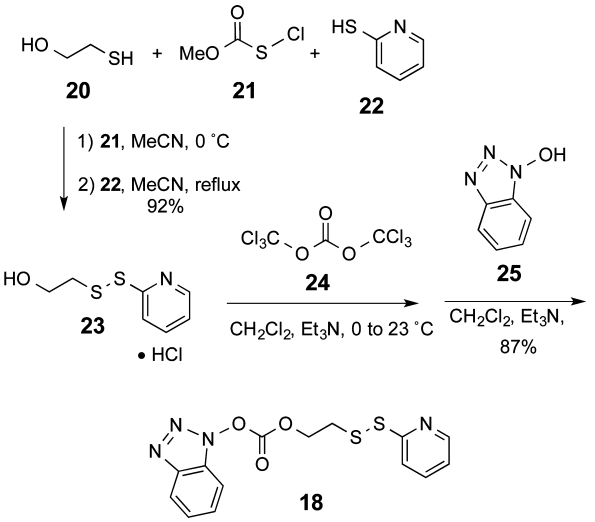

DUPA conjugates may actually be due to the very practical consideration of having the right solubility characteristics to allow adequate formulation and optimization of bioavailability at the PSMA site of action on the prostate cancer cell. The peptide nature of the linker chain will facilitate modulation of the solubility characteristics of the conjugates through substitution of different amino acid residues, and alternatively, we have already demonstrated that additional nitrogen atoms can be incorporated into the indenoisoquinoline ring system, resulting in greater aqueous solubility while maintaining Top1 inhibitory potency.[20−23] Since the disulfide moiety of the conjugate 7 is already exposed to the solvent when bound to PSMA, future drug molecules that may be attached to the left side of it in Figure 2 can presumably be exchanged without affecting the release mechanism.

EXPERIMENTAL SECTION

General. Solvents and reagents were purchased from commercial vendors and were used without further purification. Melting points were determined using capillary tubes with a Mel-Temp apparatus and are uncorrected. Infrared spectra were obtained as films on KBr pellets with $CHCl_3$ as the solvent, using a PerkinElmer 1600 series or Spectrum One FTIR spectrometer, and were baseline-corrected. ^1H NMR spectra were recorded at 300 or 500 MHz, using Bruker ARX300 or Bruker Avance 500 spectrometer with a QNP probe or TXI 5 mm/BBO probe, respectively. Mass spectral analyses were performed at the Purdue University Campus-Wide Mass Spectrometry Center. APCI-MS studies were carried out using an Agilent 6320 ion trap mass spectrometer. ESI-MS studies were performed using a FinniganMAT XL95 (FinniganMAT Corp., Bremen, Germany) mass spectrometer. The instrument was calibrated to a resolution of 10 000 with a 10% valley between peaks using the appropriate polypropylene glycol standards. MALDI-MS studies were performed using an Applied Biosystems (Framingham, MA) Voyager DE PRO mass spectrometer. This instrument utilizes a nitrogen laser (337 nm UVlaser) for ionization with a time-of-flight mass analyzer. The matrix used for these samples was 2-cyano-4-hydroxycinnamic acid, and the peptide LHRH was used as an internal standard. Analytical thin layer chromatography was carried out on Baker-flex silica gel IB2-F plastic-backed TLC plates. Compounds were visualized with both short and long wavelength UV light and ninhydrin staining unless otherwise specified. Silica gel flash column chromatography was performed using 40−63 μm flash silica gel. Solid-phase peptide synthesis (SPPS) was performed using a standard peptide synthesis apparatus (Chemglass, Vineland, NJ). All peptides and peptide conjugates were purified by

DOI: 10.1021/jm5018384
J. Med. Chem. XXXX, XXX, XXX−XXX

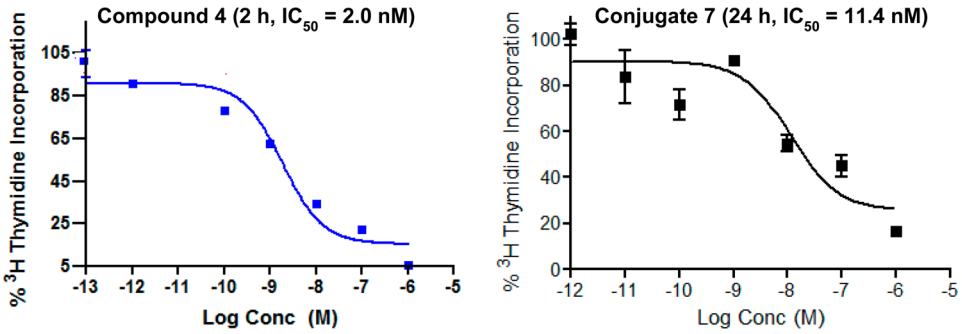

Figure 3. Dose–response ^{3}H-thymidine incorporation assays of free drug **4** and DUPA conjugate **7** on the survival of human 22RV1 cell lines after indicated incubation times.

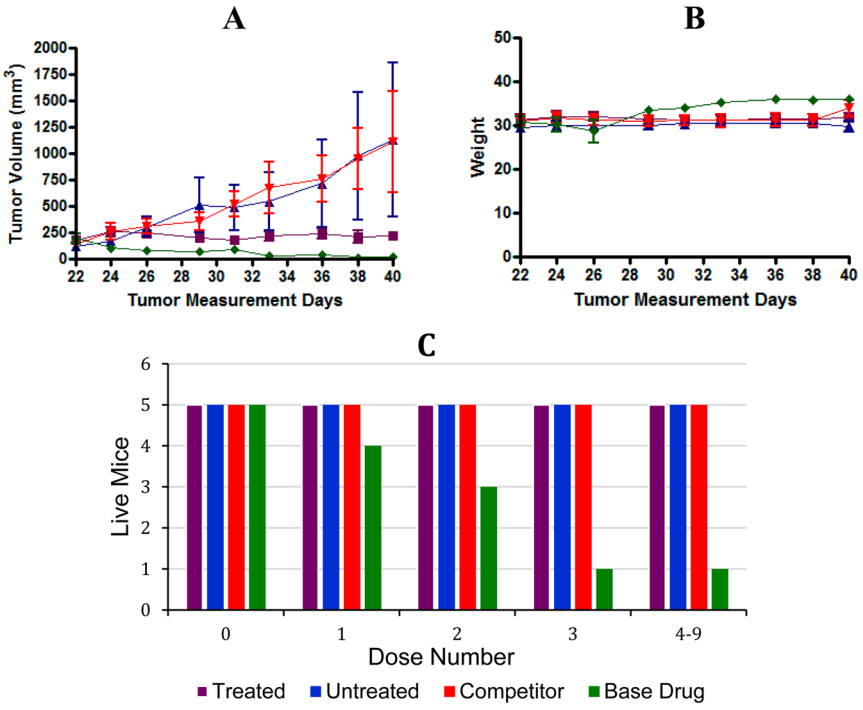

Figure 4. Animal studies with athymic nude mice bearing 22RV1 tumors: treated = **7**; untreated = saline control; competitor = **7** + **12** (100-fold excess); base drug = **4**. (A) Tumor volume vs days of therapy. (B) Average body weight vs days of therapy. (C) Live mice vs doses of therapy.

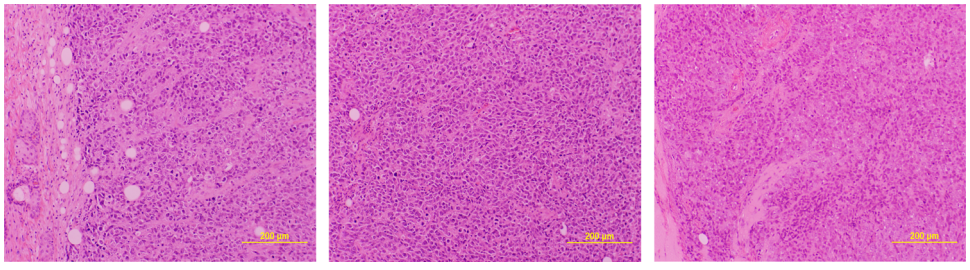

Figure 5. Histopathological aspects of PSMA-positive 22RV1 tumor. All micrographs represent H&E stains from mice treated with DUPA conjugate **7**.

preparative reverse-phase high-performance liquid chromatography (RP-HPLC; Waters, xTerra C_{18} 10 μm; 19 mm × 250 mm) and analyzed by analytical RP-HPLC (Waters 1525 binary HPLC pump with a Waters 2487 dual wavelength absorbance detector and an injection volume of 10 μL). A Sunrise C_{18} 5 μm, 100 Å reverse-phase column with dimensions of 15 cm × 4.6 mm (ES Industries) was used for all analytical HPLC experiments. For purities estimated by HPLC, the major peak accounted for ≥95% of the combined total peak area when monitored by a UV detector at 254 nm. Liquid chromatography/mass spectrometry (LC/MS) analyses were obtained using a Waters micromass ZQ 4000 mass spectrometer coupled with a UV diode array detector. All yields refer to isolated compounds.

(8*R*,11*S*,14*S*,18*S*,21*S*,34*R*,38*R*)-14-Amino-18,21-dibenzyl-11-(carboxymethyl)-1,10,13,17,20,23,31,36-octaoxo-1-((2,3,8-trimethoxy-6-(3-morpholinopropyl)-5,11-dioxo-6,11-dihydro-5*H*-indeno[1,2-c]isoquinolin-9-yl)oxy)-2-oxa-5,6-dithia-9,12,16,19,22,30,35,37-octaazatetracontane-8,34,38,40-tetracarboxylic Acid (7). Carbonate **19** (15 mg, 0.022 mmol) and DUPA–peptide reagent **12** (23 mg, 0.022 mmol) were dissolved in

DOI: 10.1021/jm5018384
J. Med. Chem. XXXX, XXX, XXX–XXX

DMSO (3 mL) and DIPEA (5.6 mg, 0.043 mmol). The mixture was stirred at room temperature for 16 h and the product was then purified by preparative RP-HPLC [λ = 280 nm; solvent gradient, 0% B to 80% B in 30 min; A = aqueous NH_4OAc/AcOH buffer at pH = 7; B = MeCN] to provide the product **7** as a plum-colored solid (22.3 mg, 63%). ^{1}H NMR (500 MHz, DMSO-d_6 + 1 drop of D_2O): δ 7.88 (s, 1 H), 7.48 (s, 1 H), 7.36 (s, 1 H), 7.22−7.06 (m, 11 H), 4.50−4.48 (m, 2 H), 4.40−4.35 (m, 5 H), 4.20 (m, 1 H), 4.09 (t, J = 5.3 Hz, 1 H), 3.83 (s, 3 H), 3.91−3.86 (m, 8 H), 3.83−3.81 (m, 3 H), 3.78 (s, 1 H), 3.40 (m, 7 H), 3.26 (m, 1 H), 3.13−3.07 (m, 2 H), 2.98 (m, 3 H), 2.93 (m, 2 H), 2.83 (m, 1 H), 2.64−2.46 (m, 3 H), 2.43 (t, J = 6.4 Hz, 1 H), 2.27 (m, 4 H), 2.18 (t, J = 7.3 Hz, 2 H), 2.04 (m, 2 H), 1.95−1.85 (m, 8 H), 1.73 (m, 2 H), 1.26 (m, 5 H), 1.07 (m, 5 H), 0.96 (m, 2 H); MALDI-MS (rel intensity) m/z 1642 (MH^+). HRMS (+ESI) calcd for MH^+ ($C_{76}H_{96}N_{11}O_{26}S_2$): 1642.5969, found 1642.6043 ($\Delta m/m$ = 4.5 ppm). UV/vis: λ_{max} = 280 nm. HPLC purity: 97.2% (MeCN, 100%).

Fmoc Solid Phase Peptide Synthesis of DUPA-Aoc-Phe-Phe-Dap-Asp-Cys Reagent (12).[15] H-L-Cys(Trt)-(2-ClTrt) resin (**11**) (0.7 mequiv/g, 200 mg, 0.14 mmol) was swollen in CH_2Cl_2 (5 mL) for 30 min, while argon was bubbled through the mixture. CH_2Cl_2 was drained, and a solution of Fmoc-L-Asp(O^tBu)-OH (2.5 equiv), PyBOP (2.5 equiv), HOBt (2.5 equiv), and DIPEA (5.0 equiv) in DMF (3 mL) was added to the resin. Argon was bubbled through the mixture for 3 h, and the solvent was then drained. The resin was washed with DMF (5 mL × 3, in 5 min/wash, drained after each wash) and ^{i}PrOH (5 mL × 3, in 5 min/wash, drained after each wash). A Kaiser test was performed to give a negative result, which indicated the coupling reaction was successful. The resin was then washed with 20% piperidine in DMF (5 mL × 3, in 10 min/wash, drained after each wash), DMF (5 mL × 3, in 5 min/wash, drained after each wash), and ^{i}PrOH (5 mL × 3, in 5 min/wash, drained after each wash). A second Kaiser test was performed to give a positive result, which indicated the cleavage of the Fmoc group was successful. The above sequence was repeated for the coupling of Boc-L-Dap(Fmoc)-OH, Fmoc-L-Phe-OH, Fmoc-L-Phe-OH, Fmoc-8-Aoc-OH, and the protected DUPA precursor **17**. The final product was cleaved from the resin by washing with a TFA/H_2O/TIPS/1,2-ethanedithiol cocktail (92.5:2.5:2.5:2.5) (7.5 mL, 30 min), during which argon was bubbled through the mixture. Another 7.5 mL portion of the cocktail was diluted with TFA (7.5 mL) to make a 15 mL solution. This solution was used to wash the resin twice (7.5 mL/wash, in 15 min/wash). The filtrate was collected and concentrated. Addition of Et_2O caused precipitation of a solid. The mixture was centrifuged, and the precipitate was collected. The crude product was purified by preparative RP-HPLC [λ = 254 nm; solvent gradient, 0% B to 80% B in 30 min; A = aqueous NH_4OAc/AcOH buffer at pH = 5; B = MeCN]. Pure fractions were combined, concentrated under vacuum, and lyophilized for 48 h to yield the pure DUPA−peptide product **12** as a white solid (172 mg, 58% overall yield, or 91.3% average yield per coupling step): mp 175−178 °C. ^{1}H NMR (300 MHz, DMSO-d_6) δ 9.39 (d, J = 9.10 Hz, 1 H), 8.92 (d, J = 8.2 Hz, 1 H), 8.68 (m, 1 H), 8.16 (m, 1 H), 7.81 (m, 1 H), 7.71 (d, J = 5.6 Hz, 1 H), 7.29−7.10, (m, 10 H), 6.45 (m, 1 H), 6.36 (m, 1 H), 4.43 (m, 4 H), 4.22 (q, J = 6.6 Hz, 3 H), 4.03−3.96 (m, 6 H), 3.43−3.36 (m, 2 H), 3.14−2.84 (m, 7 H), 2.63 (d, J = 6.6 Hz, 3 H), 2.20−2.18 (m, 2 H), 2.07 (m, 2 H), 2.02−1.94 (m, 1 H), 1.91−1.80 (m, 3 H), 1.74−1.68 (m, 3 H), 1.31−1.26 (m, 4 H), 1.17−1.03 (m, 8 H); LC/MS (ES-API) m/z 1060.2 (M^+) and 530.7 (M^{2+}). HRMS (+ESI) calcd for MH^+: 1060.4297; found, 1060.4291 ($\Delta m/m$ = 0.5 ppm). UV/vis: λ_{max} = 254 nm.

5-Benzyl 1-(*tert*-Butyl)-(((*S*)-1,5-di-*tert*-butoxy-1,5-dioxopentan-2-yl)carbamoyl)-L-glutamate (16).[15] L-Glu(O^tBu)-O^tBu (**13**) (500 mg, 1.69 mmol) and triphosgene (168 mg, 0.565 mmol) were diluted in CH_2Cl_2 (25 mL) at 0 °C in argon for 5 min, and then Et_3N (376 mg, 3.72 mmol) was added. The mixture was stirred at 0 °C for 2 h to allow isocyanate **14** formation, followed by addition of L-Glu(OBn)-O^tBu (**15**) (613 mg, 1.86 mmol) in Et_3N (244 mg, 2.42 mmol) and CH_2Cl_2 (5 mL). Stirring was continued at room temperature for 16 h, and then the reaction was quenched with 1 M HCl (50 mL). The organic layer was concentrated to a yellow syrup, which was purified by flash column chromatography, eluting with a 30−50% gradient of EtOAc in hexane, to provide the urea **16** as a clear colorless syrup (0.94 g, 96%). ^{1}H NMR (300 MHz, $CDCl_3$) δ 7.34 (s, 5 H), 5.11 (s, 2 H), 5.05−5.00 (m, 2 H), 4.40−4.31 (m, 2 H), 2.49−2.40 (m, 2 H), 2.37−2.26 (m, 2 H), 2.22- 2.05 (m, 2 H), 1.96−1.82 (m, 2 H), 1.46−1.43 (s, 27 H).

(*S*)-5-(*tert*-Butoxy)-4-(3-((*S*)-1,5-di-*tert*-butoxy-1,5-dioxopentan-2-yl)ureido)-5-oxopentanoic Acid (17).[15] Compound **16** (0.96 g, 1.66 mmol) was diluted in EtOAc (15 mL) and the mixture was degassed in 5 min with argon, followed by addition of 10% Pd on activated charcoal (20 mg), and the mixture was degassed for another 5 min. The mixture was hydrogenated at room temperature with a hydrogen balloon for 40 h and was then filtered and washed with EtOAc through a Celite pad. The solution was concentrated to provide a clear colorless syrup. The syrup was triturated with hexane and allowed to stand overnight to yield the DUPA precursor **17** as a white semisolid (0.82 g, 100%). ^{1}H NMR (300 MHz, $CDCl_3$) δ 5.84 (d, J = 8.2 Hz, 1 H), 5.42 (br s, 1 H), 4.44 (m, 1 H), 4.34 (m, 1 H), 2.43−2.39 (m, 2 H), 2.36−2.28 (m, 2 H), 2.24−2.03 (m, 2 H), 1.91−1.79 (m, 2 H), 1.48 (s, 9 H), 1.46 (s, 9 H), 1.44 (s, 9 H).

1*H*-Benzo[*d*][1,2,3]triazol-1-yl[2-(pyridin-2-yldisulfanyl)-ethyl] Carbonate (18).[13] Compound **23** (1.00 g, 4.47 mmol) was dissolved in CH_2Cl_2 (5 mL) and Et_3N (0.45 g, 4.47 mmol) and added dropwise to a solution of triphosgene (**24**) (0.44 g, 1.49 mmol) at 0 °C. The solution was stirred at room temperature for 1.5 h, followed by dropwise addition of a solution of hydroxybenzotriazole (**25**) (0.60 g, 4.47 mmol) in CH_2Cl_2 (10 mL) and Et_3N (0.45 g, 4.47 mmol). The mixture was then stirred at room temperature for 16 h and then diluted with $CHCl_3$ to 50 mL and washed with H_2O (100 mL × 3) and brine (100 mL). The organic layer was dried over anhydrous Na_2SO_4, filtered, and concentrated. The resulting yellow oil was triturated with hexane and filtered to provide the product **18** as a white solid (1.36 g, 87%): mp 116−118 °C. ^{1}H NMR (300 MHz, $CDCl_3$) δ 8.40 (d, J = 4.8 Hz, 1 H), 8.18 (d, J = 8.4 Hz, 1 H), 8.04 (d, J = 8.4 Hz, 1 H), 7.92 (t, J = 8.0 Hz, 1 H), 7.77−7.74 (m, 2 H), 7.66 (t, J = 7.8 Hz, 1 H), 7.19 (m, 1 H), 4.74 (t, J = 6.0 Hz, 2 H), 3.38 (t, J = 6.0 Hz, 2 H).

2-(Pyridin-2-yldisulfanyl)ethyl (2,3,8-Trimethoxy-6-(3-morpholinopropyl)-5,11-dioxo-6,11-dihydro-5*H*-indeno[1,2-c]-isoquinolin-9-yl) Carbonate (19). Compound **4** (50 mg, 0.10 mmol) was dissolved in CH_2Cl_2 (5 mL), followed by addition of carbonate reagent **18** (48 mg, 0.12 mmol), DMAP (13 mg, 0.10 mmol), and Et_3N (21 mg, 0.21 mmol). The mixture was stirred at room temperature for 16 h and was then loaded directly onto a silica gel column and purified by flash column chromatography, eluting with 3% MeOH in $CHCl_3$, to provide the product **19** as a red solid (64.8 mg, 90%): mp 130−132 °C. ^{1}H NMR (300 MHz, $CDCl_3$) δ 8.51 (d, J = 4.5 Hz, 1 H), 8.09 (s, 1 H), 7.69−7.66 (m, 3 H), 7.37 (s, 1 H), 7.16−7.12 (m, 2 H), 4.59 (q, J = 6.6 Hz, 4 H), 4.06 (s, 3 H), 4.00 (s, 3 H), 3.98 (s, 3 H), 3.68 (t, J = 4.3 Hz, 4 H), 3.18 (t, J = 6.5 Hz, 2 H), 2.59 (t, J = 6.9 Hz, 2 H), 2.47 (br s, 4 H), 2.14 (m, 2 H).

2-(Pyridin-2-yldisulfanyl)ethanol Hydrochloride (23).[13] 2-Mercaptoethanol (**20**) (0.77 g, 9.9 mmol) was dissolved in CH_3CN (5 mL), and the solution was added dropwise to a solution of methoxycarbonylsulfenyl chloride (**21**) (1.25 g, 9.9 mmol) in CH_3CN (8 mL) precooled at 0 °C. The pale yellow solution was stirred at 0 °C for 30 min until it turned colorless. A solution of 2-mercaptopyridine (**22**) (1.0 g, 9.0 mmol) in CH_3CN (20 mL) was added dropwise to the clear solution, and the yellow mixture was stirred at reflux for 2 h, during which a white precipitate formed. The colorless mixture with white precipitate was then stirred at 0 °C for 1 h and filtered. The filter cake was washed with CH_3CN to provide the product **23** as a white amorphous solid (1.84 g, 92%): mp 128−130 °C. ^{1}H NMR (300 MHz, $CDCl_3$) δ 9.13 (d, J = 5.5 Hz, 1 H), 8.10 (t, J = 7.4 Hz, 1 H), 7.82 (d, J = 8.3 Hz, 1 H), 7.61 (t, J = 6.6 Hz, 1 H), 4.01 (t, J = 5.2 Hz, 2 H), 3.27 (t, J = 5.6 Hz, 2 H); ESI-MS (positive mode) m/z (rel intensity) 188 [$(MH - H_2O)^+$, 100].

General Procedure for IC_{50} (Dose Dependence) Studies. 22RV1 cells were seeded in 24-well (50 000 cells/well) Falcon plates and allowed to form monolayers over a period of 24−48 h. The old medium was replaced with fresh medium (0.5 mL) containing increasing concentrations of drug (either targeted or nontargeted), and

DOI: 10.1021/jm5018384
J. Med. Chem. XXXX, XXX, XXX−XXX

cells were incubated for an additional 2 h (in the case of **4**) or 2 and 24 h (in the case of the targeted drug **7**) at 37 °C. Cells were washed (3 × 0.5 mL) with fresh medium and incubated in fresh medium (0.5 mL) for another 66 h at 37 °C. The spent medium in each well was replaced with fresh medium (0.5 mL) containing ^{3}H-thymidine (1 mCi/mL), and the cells were incubated for an additional 4 h at 37 °C to allow ^{3}H-thymidine incorporation. The cells were then washed with medium (2 × 0.5 mL) and treated with 5% trichloroacetic acid (0.5 mL) for 10 min at room temperature. The trichloroacetic acid was replaced with 0.25 N NaOH (0.5 mL), and the cells were transferred to individual scintillation vials containing Ecolume scintillation cocktail (3.0 mL), mixed well to form homogeneous liquid, and counted in a liquid scintillation analyzer. IC_{50} values were calculated by plotting the percentage of ^{3}H-thymidine incorporation versus log concentration of drugs (targeted and nontargeted) by using GraphPad Prism 4.

In Vivo Experiment. All procedures performed on live mice were approved by the Purdue Animal Use and Care Committee and conformed with NIH guidelines. Five- to six-week-old male nu/nu mice (Harlan Laboratories) were maintained on a standard 12 h light−dark cycle and fed on normal mouse chow for the duration of the experiment. PSMA-positive prostate cancer 22RV1 cells (2×10^{6} in 20% HC Matrigel) were injected in the right shoulders of the mice. Tumors were measured in two perpendicular directions every 2−3 days with vernier calipers, and their volumes were calculated as $0.5 \times L \times W^{2}$ where L is the longest axis (in millimeters) and W is the axis perpendicular to L (in millimeters). Dosing solutions of the test compound were prepared in sterile saline and administered in mice via ip injection. Mice were divided into four groups (5 mice/group), and treatments were initiated when the subcutaneous tumors reached ∼100 mm^{3} in volume. Each dose was given at 2 μmol/kg of the test compound in a volume of 100 μL of saline. As a measure of gross toxicity, mouse weights were also recorded at each dosing. Results were plotted by using GraphPad Prism 4.

Histological Staining. Tumors were excised, sectioned, and stained with hematoxylin and eosin by the Purdue Histology and Phenotyping Laboratory.

■ ASSOCIATED CONTENT

Ⓢ Supporting Information

SMILES molecular formula strings in csv format. This material is available free of charge via the Internet at http://pubs.acs.org.

■ AUTHOR INFORMATION

Corresponding Author

*Phone: 765-494-1465. Fax: 765-494-6970. E-mail: cushman@purdue.edu.

Author Contributions

§J.R. and T.X.N. contributed equally to this work.

Notes

The authors declare the following competing financial interest(s): Mark Cushman is on the Board of Directors and is an investor in Linus Oncology, Inc., which has licensed indenoisoquinoline intellectual property owned by Purdue University. Neither Linus Oncology, Inc., nor any other commercial company sponsored or provided other direct financial support to the author or his laboratory for the research reported in this article. The remaining authors have no competing and/or relevant financial interest(s) to disclose.

■ ACKNOWLEDGMENTS

This work was made possible by the National Institutes of Health (NIH) through support with Research Grants UO1 CA023168 and P30 CA023168. This research was also supported in part by the Floss Endowment Fellowship from the Department of Medicinal Chemistry at Purdue University.

■ ABBREVIATIONS USED

CPT, camptothecin; DMSO-d_6, dimethyl-d_6 sulfoxide; DUPA, 2-[3-(1,3-dicarboxypropyl)ureido]pentanedioic acid; ESI-MS, electrospray ionization mass spectrometry; HRMS, high resolution mass spectrometry; LC/MS, liquid chromatography/mass spectrometry; MALDI-MS, matrix-assisted laser desorption ionization mass spectrometry; MGM, mean-graph midpoint; PSMA, prostate-specific membrane antigen; RP-HPLC, reverse-phase high-performance liquid chromatography; Top1, human topoisomerase type IB

■ REFERENCES

(1) Siegel, R.; Ma, J. M.; Zou, Z. H.; Jemal, A. Cancer Statistics, 2014. *Ca—Cancer J. Clin.* **2014**, *64*, 9−29.

(2) Soudy, R.; Chen, C.; Kaur, K. Novel Peptide-Doxorubucin Conjugates for Targeting Breast Cancer Cells Including the Multidrug Resistant Cells. *J. Med. Chem.* **2013**, *56*, 7564−7573.

(3) Kumar, S. J.; Barqawi, A.; Crawford, D. Advere Events Associated with Hormonal Therapy for Prostate Cancer. *Adv. Urol.* **2005**, *7* (Suppl. 5), S37−S43.

(4) O'Keefe, D. S.; Bacich, D. J.; Heston, W. D. W. Comparative Analysis of Prostate-Specific Membrane Antigen (PSMA) versus a Prostate-Specific Membrane Antigen-like Gene. *Prostate* **2004**, *58*, 200−210.

(5) Troyer, J. K.; Beckett, M. L.; Wright, G. L. Detection and Characterization of the Prostate-Specific Membrane Antigen (PSMA) in Tissue-Extracts and Body-Fluids. *Int. J. Cancer* **1995**, *62*, 552−558.

(6) Carter, R. E.; Feldman, A. R.; Coyle, J. T. Prostate-Specific Membrane Antigen Is a Hydrolase with Substrate and Pharmacologic Characteristics of a Neuropeptidase. *Proc. Natl. Acad. Sci. U.S.A.* **1996**, *93*, 749−753.

(7) Warg, X.; Yin, L.; Rao, P.; Stein, R.; Harsch, K. M.; Lee, Z.; Heston, W. D. W. Targeted Treatment of Prostate Cancer. *J. Cell. Biochem.* **2007**, *102*, 571−579.

(8) Ghosh, A.; Heston, W. D. W. Tumor Target Prostate Specific Membrane Antigen (PSMA) and Its Regulation in Prostate Cancer. *J. Cell. Biochem.* **2004**, *91*, 528−539.

(9) Chang, S. S.; O'Keefe, D. S.; Bacich, D. J.; Reuter, V. E.; Heston, W. D. W.; Gaudin, P. B. Prostate-Specific Membrane Antigen Is Produced in Tumor-Associated Neovasculature. *Clin. Cancer Res.* **1999**, *5*, 2674−2681.

(10) Kozikowski, A. P.; Zhang, J.; Nan, F. J.; Petukhov, P. A.; Grajkowska, E.; Wroblewski, J. T.; Yamamoto, T.; Bzdega, T.; Wroblewska, B.; Neale, J. H. Synthesis of Urea-Based Inhibitors as Active Site Probes of Glutamate Carboxypeptidase II: Efficacy as Analgesic Agents. *J. Med. Chem.* **2004**, *47*, 1729−1738.

(11) Kozikowski, A. P.; Nan, F.; Conti, P.; Zhang, J. H.; Ramadan, E.; Bzdega, T.; Wroblewska, B.; Neale, J. H.; Pshenichkin, S.; Wroblewski, J. T. Design of Remarkably Simple, Yet Potent Urea-based Inhibitors of Glutamate Carboxypeptidase II (NAALADase). *J. Med. Chem.* **2001**, *44*, 298−301.

(12) Liu, H.; Rajasekaran, A. K.; Moy, P.; Xia, Y.; Kim, S.; Navarro, V.; Rahmati, R.; Bander, N. H. Constitutive and Antibody-Induced Internalization of Prostate-Specific Membrane Antigen. *Cancer Res.* **1998**, *58*, 4055−4060.

(13) Kularatne, S. A.; Venkatesh, C.; Santhapuram, H. K. R.; Wang, K.; Vaitilingam, B.; Henne, W. A.; Low, P. S. Synthesis and Biological Analysis of Prostate-Specific Membrane Antigen-Targeted Anticancer Prodrugs. *J. Med. Chem.* **2010**, *53*, 7767−7777.

(14) Kularatne, S. A.; Wang, K.; Santhapuram, H. K. R.; Low, P. S. Prostate-Specific Membrane Antigen Targeted Imaging and Therapy of Prostate Cancer Using a PSMA Inhibitor as a Homing Ligand. *Mol. Pharmaceutics* **2009**, *6*, 780−789.

(15) Kularatne, S. A.; Zhou, Z. G.; Yang, J.; Post, C. B.; Low, P. S. Design, Synthesis, and Preclinical Evaluation of Prostate-Specific Membrane Antigen Targeted ^{99m}Tc-Radioimaging Agents. *Mol. Pharmaceutics* **2009**, *6*, 790−800.

DOI: 10.1021/jm5018384
J. Med. Chem. XXXX, XXX, XXX−XXX

(16) Mesters, J. R.; Barinka, C.; Li, W. X.; Tsukamoto, T.; Majer, P.; Slusher, B. S.; Konvalinka, J.; Hilgenfeld, R. Structure of Glutamate Carboxypeptidase II, a Drug Target in Neuronal Damage and Prostate Cancer. *EMBO J.* **2006**, *25*, 1375−1384.
(17) Cinelli, M. A.; Reddy, P. V. N.; Lv, P. C.; Liang, J. H.; Chen, L.; Agama, K.; Pommier, Y.; van Breemen, R. B.; Cushman, M. Identification, Synthesis, and Biological Evaluation of Metabolites of the Experimental Cancer Treatment Drugs Indotecan (LMP400) and Indimitecan (LMP776) and Investigation of Isomerically Hydroxylated Indenoisoquinoline Analogues as Topoisomerase I Poisons. *J. Med. Chem.* **2012**, *55*, 10844−10862.
(18) Leamon, C. P.; Reddy, J. A.; Vetzel, M.; Dorton, R.; Westrick, E.; Parker, N.; Wang, Y.; Vlahov, I. Folate Targeting Enables Durable and Specific Antitumor Responses from a Therapeutically Null Tubulysin B Analogue. *Cancer Res.* **2008**, *68*, 9839−9844.
(19) Fujiwara, Y.; Akaji, K.; Kiso, Y. Racemization-Free Synthesis of C-Terminal Cysteine-Peptide using 2-Chlorotrityl Resin. *Chem. Pharm. Bull.* **1994**, *42*, 724−726.
(20) Kiselev, E.; Dexheimer, T. S.; Pommier, Y.; Cushman, M. Design, Synthesis, and Evaluation of Dibenzo[*c*,*h*][1,6]naphthyridines as Topoisomerase I Inhibitors and Potential Anticancer Agents. *J. Med. Chem.* **2010**, *53*, 8716−8726.
(21) Kiselev, E.; DeGuire, S.; Morrell, A.; Agama, K.; Dexheimer, T. S.; Pommier, Y.; Cushman, M. 7-Azaindenoisoquinolines as Topoisomerase I Inhibitors and Potential Anticancer Agents. *J. Med. Chem.* **2011**, *54*, 6106−6116.
(22) Kiselev, E.; Agama, K.; Pommier, Y.; Cushman, M. Azaindenoisoquinolines as Topoisomerase I Inhibitors and Potential Anticancer Agents: A Systematic Study of Structure-Activity Relationships. *J. Med. Chem.* **2012**, *55*, 1682−1697.
(23) Kiselev, E.; Empey, N.; Agama, K.; Pommier, Y.; Cushman, M. Dibenzo[*c*,*h*][1,5]naphthyridinediones as Topoisomerase I Inhibitors: Design, Synthesis, and Biological Evaluation. *J. Org. Chem.* **2012**, *77*, 5167−5172.

DOI: 10.1021/jm5018384
J. Med. Chem. XXXX, XXX, XXX−XXX